Application of Kogelnik's two-wave theory to deep, slanted, highly efficient, relief transmission gratings

Hendrik J. Gerritsen, Donald K. Thornton, and Sarah R. Bolton

Deep photoresist gratings, slanted as well as unslanted, were produced holographically in clear Shipley 1400 photoresist. The diffraction efficiencies of these gratings were measured as a function of incident angle for three wavelengths with polarization perpendicular to the plane of incidence. It is shown that the results agree fairly well with those predicted by Kogelnik's two-wave theory, indicating that these relief gratings behave like volume holograms. An explanation in terms of thin and thick gratings is given, and practical conclusions are drawn from these observations.

I. Introduction

It is not generally appreciated that relief transmission gratings, containing groove spacings and groove depths of about one wavelength of visible light—as the gratings described here—behave rather closely like volume gratings. They have maximum efficiencies near 100%, Bragg angle selectivity, and they mainly exhibit two transmitted beams, the zeroth and one first-order beam, just like volume holograms. One reason this fact is not widely known, outside a small group of specialists, is a result of a discussion of sinusoidal phase gratings in an early influential book on holography.[1]

The authors derive that such gratings have a maximum first-order diffraction efficiency of only 33.9% and no Bragg angle selectivity. They quote results of a holographically etched photoresist film and show that it behaves as a typical example of a thin phase grating. In fact, early photoresist gratings, used mainly to produce images, had experimentally determined efficiencies near 10%.[2] This has led many workers in the field to believe that photoresist gratings cannot be expected to have large diffraction efficiencies. The purpose of this paper is to show that this generalization cannot be made and that, moreover, Kogelnik's two-wave coupled theory[3] is quite applicable in detail to deep, narrowly spaced photoresist gratings.

The writers are aware of and will later discuss rather recent experiments on photoresist gratings which indicate[4–6] that deep gratings cannot be considered as thin phase gratings because of their large efficiency, and a considerable body of careful theoretical discussions on the thin vs thick issue exists[7–9] to which we will come back shortly. We apply Kogelnik's theory to our data, realizing that this stretches the range of validity of the theory. The results validate this approach, we believe. At the same time, we hope to demonstrate that large diffraction efficiencies are obtainable over a broad range of angles and wavelengths and that the response curves can be shifted by making a slanted grating, all in fair agreement with Kogelnik's theoretical predictions for volume diffraction gratings.

A more complex but exact theory has been developed[10–12] for various grating profiles, but so far only the maximum efficiency of these gratings has been calculated, not the angular or wavelength dependence of the efficiency. This theory also predicts efficiencies in the 90% range in agreement with earlier experiments[4–6] and this paper.

The great advantage of using the coupled two-wave theory[3,13] is its computational simplicity and the wide range of variation in the parameters it allows.

II. Grating Fabrication and Characterization

The relief gratings used in the experiments were recorded holographically in Shipley AZ 1400-31 positive photoresist, spin coated on 2.54 × 7.6-cm (1 × 3-in.) cleaned microscope slides. After spinning for 10 s at the slow speed of 2000 rpm and baking for 0.5 h at 80°C, a 2–3-μm thick photoresist layer was obtained, sufficiently thick to serve as a substrate for the deep holographic gratings.

When this work was done all authors were with Brown University, Physics Department, Providence, Rhode Island 02912; Sarah Bolton is now with the University of California at Berkeley, Physics Department, Berkeley, California 94705.

Received 12 March 1990.
0003-6935/91/070807-08$05.00/0.

The gratings were produced by placing the photoresist coated slides in the interference pattern of two plane waves of 458 nm and 50-mW power, obtained from a 95-4 Lexel argon ion laser. The total light intensity was ~0.25 mW/cm^2 at the slide. With 20–30-min exposure this resulted in an amount of energy of 0.3 J/cm^2 on the photoresist surface. The slides were index matched on the back side with xylene, which formed a thin layer between the slide and a black absorber. This was done to prevent back reflections. Three different gratings will be described: grating 1, in which both incident beams in air made an angle of ±21.5° with the substrate normal, leading to an unslanted grating; grating 2, a shallower unslanted grating in which the angles were ±27°; and grating 3, in which the two beams made angles of +48 and −6° with the substrate normal to produce a slanted grating.

After exposure, the slides were developed in dilute Shipley microposit developer (1 part developer with 2 parts water) for 1–3 min to obtain maximum brightness of diffraction. Development was stopped by plunging the grating into distilled water, which was followed by air drying and 5-min exposure to a 300-W UV blacklight at a wavelength of 365 nm. The latter step converts the yellowish photoresist to a virtually colorless state. This is important to reduce absorption and allows one to treat the gratings as essentially lossless. Measurements of a 2.5-μm thick photoresist layer thus treated—but without diffraction grating—had only 1% absorption at 633 nm, 5% at 543 nm, and 8% at 442 nm. Since the grating depth for all diffraction gratings studied here is <0.6 μm, the absorption in the actual grating is thus at most 2%, although the layer of photoresist under the actual grating will, of course, still absorb a small fraction of the light.

The three gratings were characterized and measured in various ways. Electron microscope photographs of cross sections of the gratings gave the grating spacing, the grating depth (the distance from top to bottom), and the grating slant angle. The other type of characterization were the optical measurements of the intensities of the various beams observed. Three measurement wavelengths were chosen; namely, 633, 514, and 458 nm using laser beams of ~3 mW incident on the grating side of each sample with the electric field polarized perpendicular to the plane of incidence. The same small area of the grating was used for all the measurements to avoid possible profile variations, and the readings were taken as a function of incident angle.

III. Electron Microscope Results

Figures 1–3 show the electron microscope photographs of the unslanted and slanted cross sections, respectively. The cross sections were obtained from the same area where the optical data were taken by scoring the backside of the slide with a carbide glass pen where the optical data had been taken, and snapping the slide at that area. The expected grating spacing Λ is given by $\Lambda = \lambda/(2\sin\alpha)$ where λ = 458 nm and α = 21.5 and 27° for the unslanted gratings. This results in Λ = 625 nm and 504 nm. Since no very accurate calibration of magnification of the electron microscope was available, these values were used to derive the top-to-bottom distances. We derived from the figure the values of 620 and 342 ± 20 nm for this parameter d, the grating thickness.

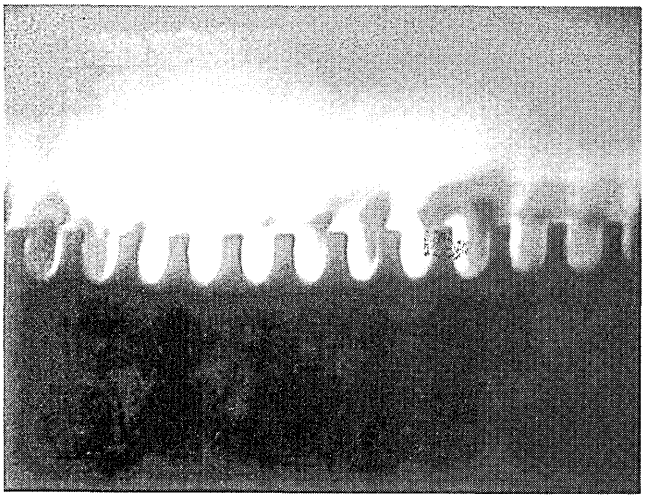

Fig. 1. Grating 1: Λ = grating spacing = 625 nm; d = grating depth = 620 nm.

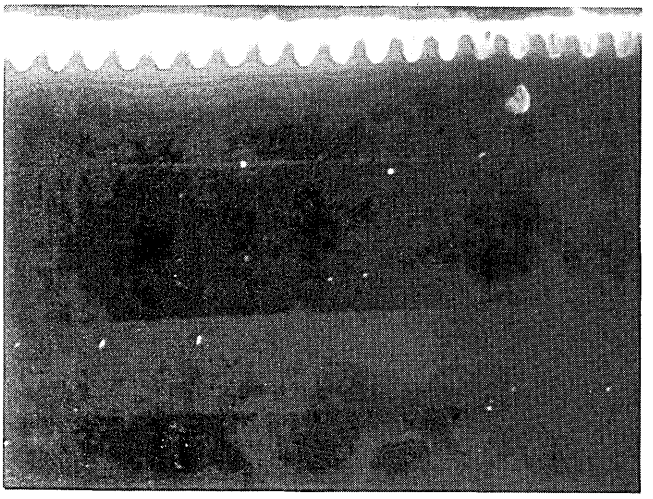

Fig. 2. Grating 2: Λ = grating spacing = 504 nm; d = grating depth = 342 nm.

For the slanted grating, grating 3, made with external angles (in air) of 48 and 6°, one calculates for $\Lambda = \lambda/(\sin 48° + \sin 6°)$ = 540 nm. Assuming this to be the grating spacing in the electron microscope pictures leads to a top-to-bottom distance of 540 ± 15 nm for the slanted grating. The measured slant angle χ (see Fig. 3a) is 12 ± 0.5° while the calculated slant angle is 11.5°. This follows from computing the internal angles, $\sin 48°/1.66 = \sin\alpha_i$ and $\sin 6°/1.66 = \sin\beta_i$ and taking as slant angle, $\chi, \chi = (\alpha_i + \beta_i)/2 - \beta_i$. The refractive index of the photoresist in the visible is taken as 1.66.[14] Figures 1–3(a) and 3(b) show electron microscope cross sections of the gratings. The photoresist shows up black in these photographs. The shape is similar to that reported in Refs. 5 and 6. Note that

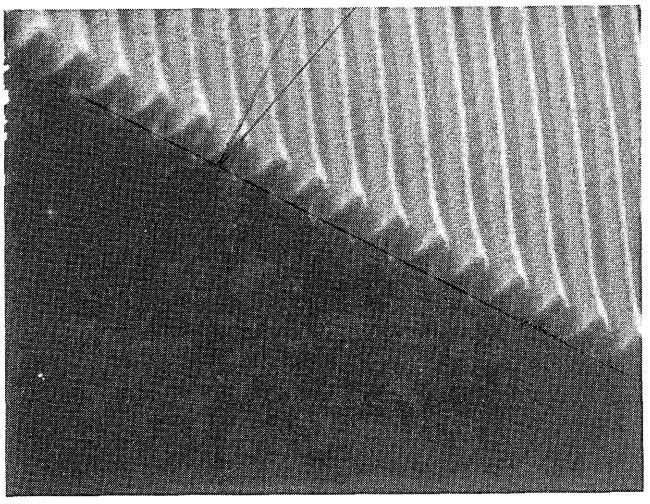

(a)

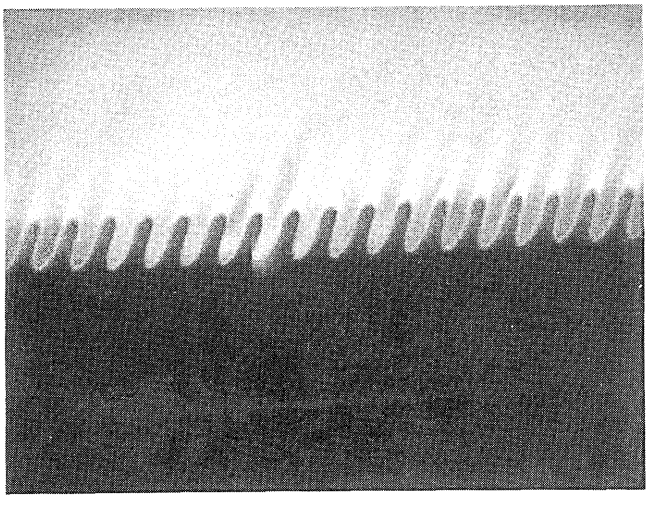

(b)

Fig. 3. (a) Grating 3: Λ = grating spacing = 540 nm; d = grating depth = 540 nm; slant angle = 12 ± 0.5°. (b) Grating 3: profile detail of slanted grating.

the shallower grating 2 has a more sinusoidal profile than the deeper gratings.

IV. Optical Measurements Procedure

The gratings were measured in collimated laser light of an incident intensity of 3 mW at the wavelengths of 633, 514, and 458 nm, which always entered from the grating side. The various reflected and refracted beams were measured with a Liconix 45 PM light meter. Most data were taken with the electric field polarization of the laser beams perpendicular to the plane of incidence, which makes it parallel to the diffracting grooves. This case is slightly easier to treat theoretically and is used in Kogelnik's paper, although the case of parallel polarization can readily be analyzed as shown in the Appendix of Kogelnik's paper. These data will not be presented here but they were also in general agreement with theory.

The intensities of the incident, diffracted, and reflected beams were measured as a function of incident angle for each of three wavelengths in the visible spectrum.

The measured data and theoretical curves for grating 1 are shown in graphs 4–9; for grating 2, in graphs 10–15, and for grating 3, in graphs 16–21. Included in the graphs is a curve meandering between 0.75 and 0.95. It represents the fraction of the incident light that we could account for as the sum total of the intensity of all the beams measured. The relatively small fraction of missing power is believed to be lost through absorption in the layer (up to 8% in the violet), scattering, and sometimes wave guiding, by which we mean that propagation may take place in the plane of the substrate due to the slight mismatch of refractive indices between photoresist and glass. For some orientations we could actually observe some light being propagated that way and leaving the side of the substrate. That happened particularly near angles where orders other than the first order would be diffracted close to parallel to the substrate. No further work was done to track down or reduce this missing 15% ± 5% and the data were subsequently corrected for it to compare them with the theoretical predictions as explained in the next section.

V. Data Analysis

As indicated in Sec. I, we have applied Kogelnik's two-coupled-wave theory to our data after correcting the data for absorption, scatter, and reflection losses. This correction is necessary because Kogelnik's theory only studies the interplay between the incident beam, the periodic grating, and one diffracted beam inside the medium and ignores any reflection. In practice one can reduce reflections, if needed, by applying antireflex coatings to the interfaces. We first explain how the correction was made.

We argue that the lost light should be distributed over the various beams in ratio of the observed intensity of this beam. This seems obvious for losses from absorption and scattering. Furthermore, we have to correct for reflection of the zeroth-order beam. If, for example, 10% of it is reflected on incidence, obviously the diffracted beam will be 10% weaker than without that reflection. To correct the first-order diffracted beam—the only beam for which we did the correction since it is the one we want to compare with theory—we use the following formula:

$$I^{+1}_{\text{corrected}} = \frac{I^{+1}}{\text{fraction of light accounted for}} + I^{+1}_{\text{reflected}} + I^{0}_{\text{reflected}}\left(\frac{I^{+1} + I^{+1}_{\text{reflected}}}{I^{0} + I^{+1} + I^{+1}_{\text{reflected}}}\right),$$

in which I^{+1} represents the measured intensity of the strong first-order diffracted beam and I^{0} that of the zeroth-order beam. It is likely that the corrected values should be reduced somewhat, which would bring them on, or slightly below, the theoretical curves.

The keys to the symbols used are shown in Figs. 4 and 5. While in Fig. 4 no orders other than the 0 and +1, and their reflections, have significant intensity, for

EXPERIMENTAL DATA in RED (633 nm), λ = 625 nm, d = 620 nm

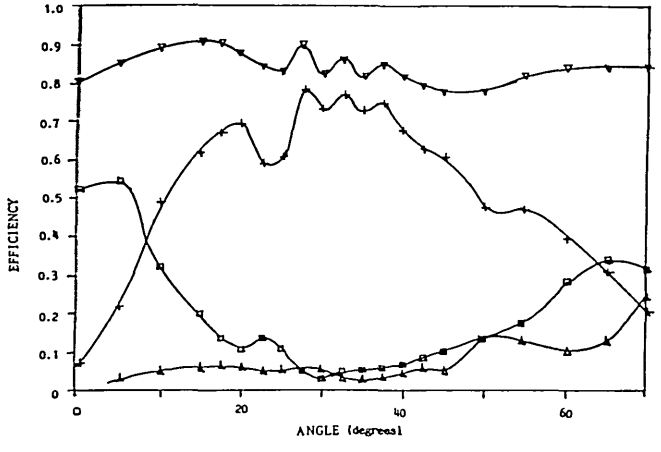

Fig. 4 Grating 1 □ = zeroth order transmitted, △ = zeroth order reflected, + = first order, ▽ = total light measured

EXPERIMENTAL DATA in GREEN (514 nm)

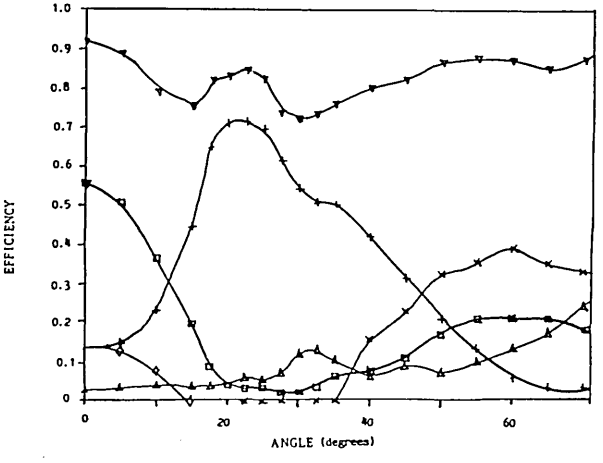

Fig 5 Grating 1 □ = zeroth order transmitted, △ = zeroth order reflected, + = first order, × = second order, ◇ = -1th order, ▽ = total light measured

EXPERIMENTAL DATA in BLUE (458 nm)

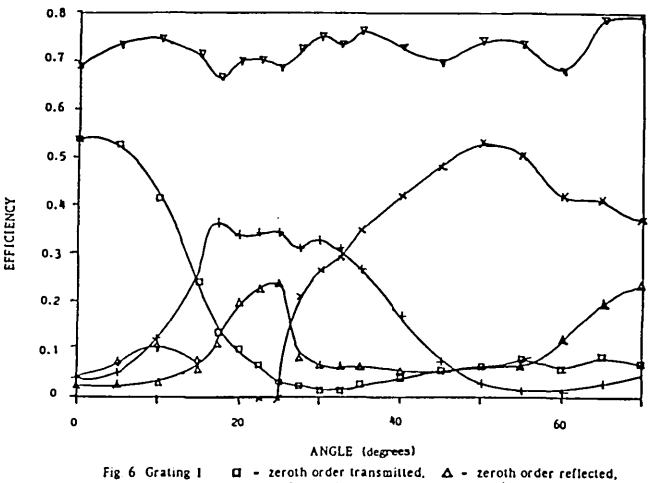

Fig 6 Grating 1 □ = zeroth order transmitted, △ = zeroth order reflected, + = first order, × = second order, ◇ = -1th order, ▽ = total light measured

THEORY VERSUS EXPERIMENT in RED (633 nm), λ = 625 nm, d = 620 nm, n = 1.66

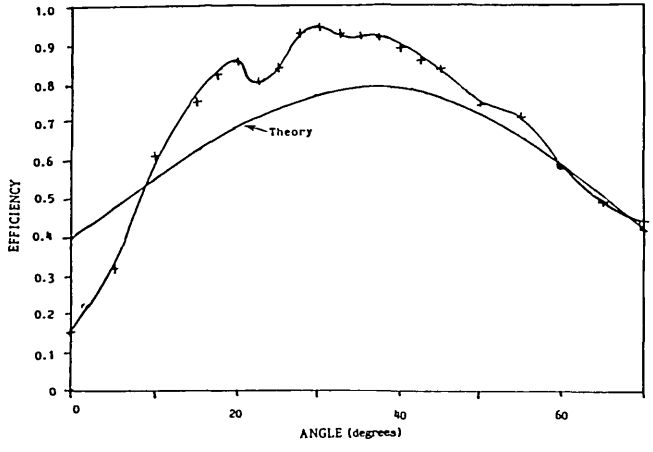

Fig. 7 Grating 1 + = experimental (corrected) 1st order

THEORY VERSUS EXPERIMENT in GREEN (514 nm)

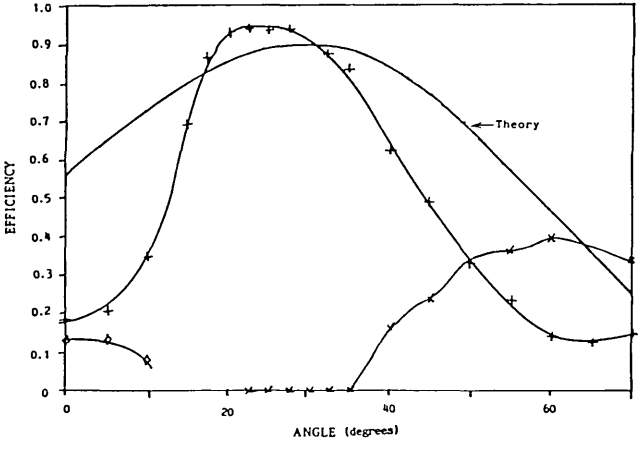

Fig. 8 Grating 1 + = experimental (corrected) 1st order, × = second order, ◇ = -1st order

THEORY VERSUS EXPERIMENT in BLUE (458 nm)

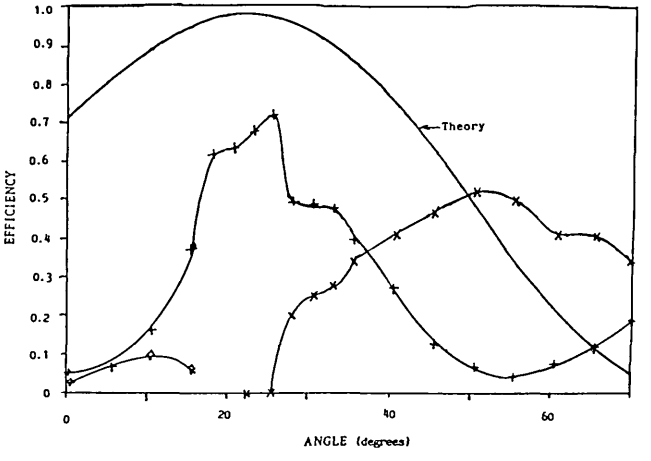

Fig. 9 Grating 1 + = experimental (corrected) 1st order, × = second order, ◇ = -1st order

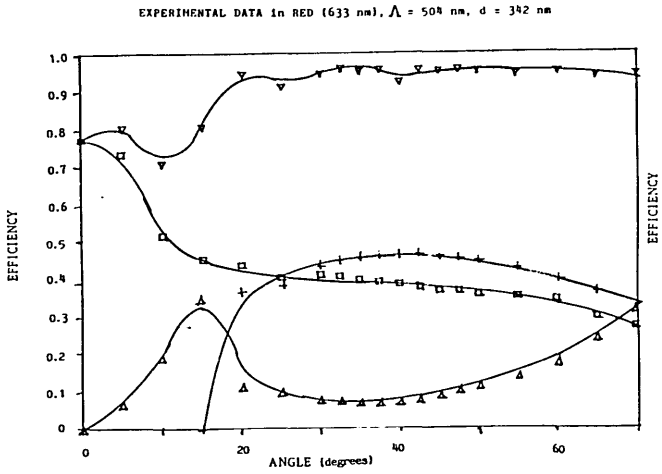

Fig. 10 Grating 2 □ - zeroth order transmitted, △ - zeroth order reflected, + - first order, ▽ - total light measured

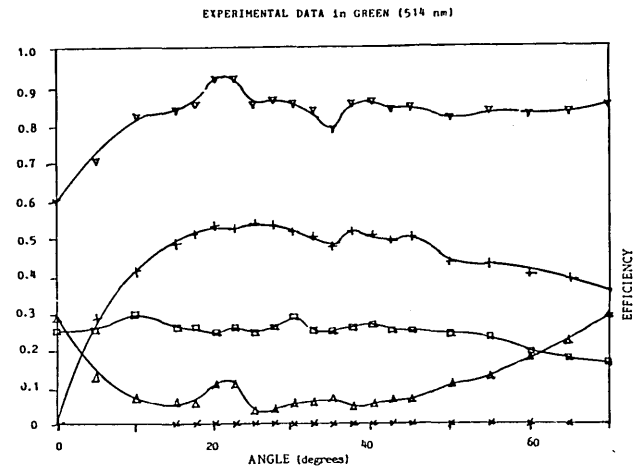

Fig. 11 Grating 2 □ - zeroth order transmitted, △ - zeroth order reflected, + - first order, × - second order, ▽ - total light measured

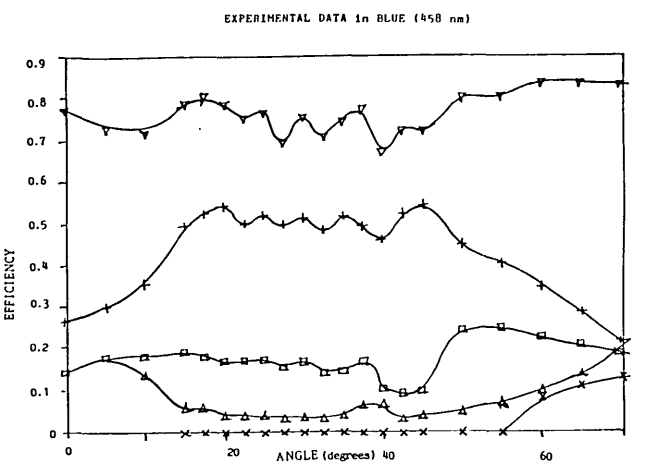

Fig. 12 Grating 2 □ - zeroth order transmitted, △ - zeroth order reflected, + - first order, × - second order, ▽ - total light measured

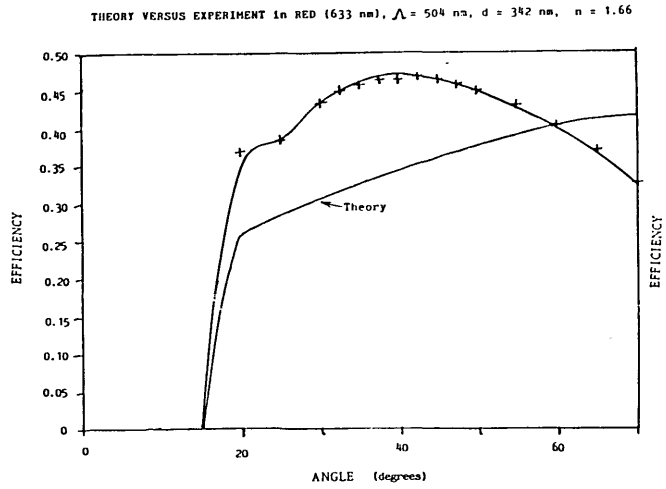

Fig. 13 Grating 2 + - experimental (corrected) 1st order

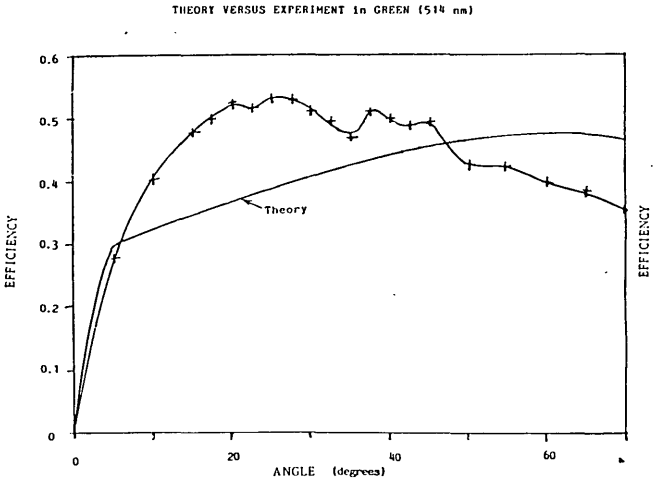

Fig. 14 Grating 2 + = experimental (corrected) 1st order

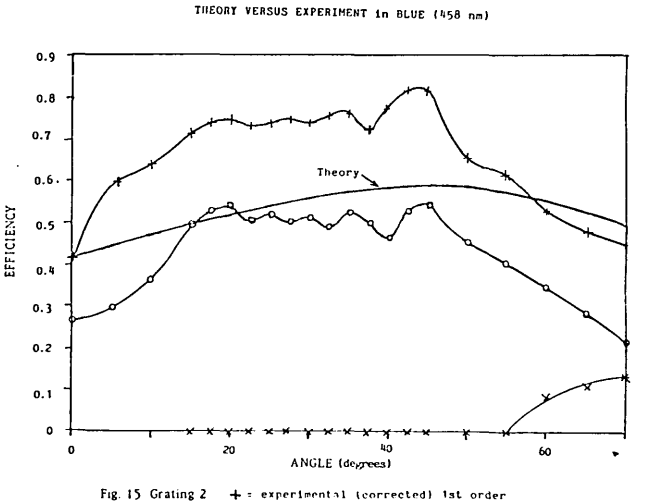

Fig. 15 Grating 2 + = experimental (corrected) 1st order, × - second order, o = experimental 1st order

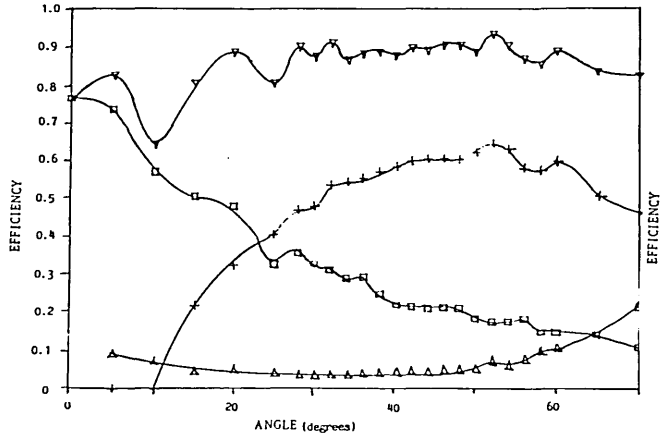

Fig. 16 Grating 3 □ - zeroth order transmitted, Δ - zeroth order reflected, + - first order, ▽ - total light measured

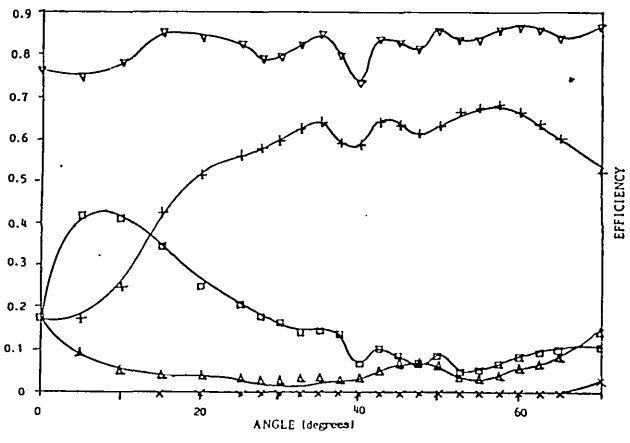

Fig 17 Grating 3 □- zeroth order transmitted, Δ- zeroth order reflected, +- first order, ×- second order, ▽- total light measured

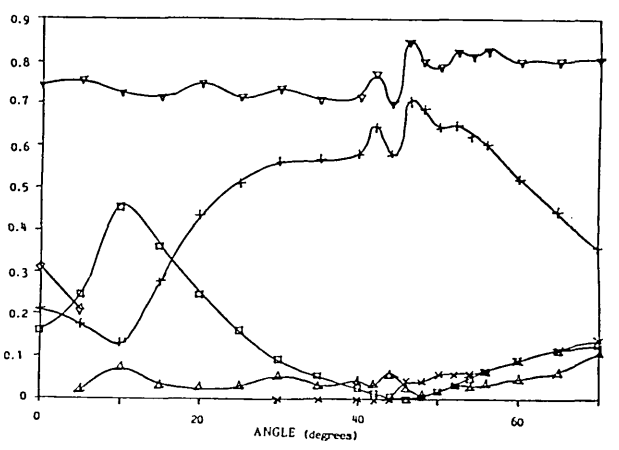

Fig. 18 Grating 3 □ - zeroth order transmitted, Δ - zeroth order reflected, + - first order, × - second order, ◊ - -1st order, ▽ - total light measured

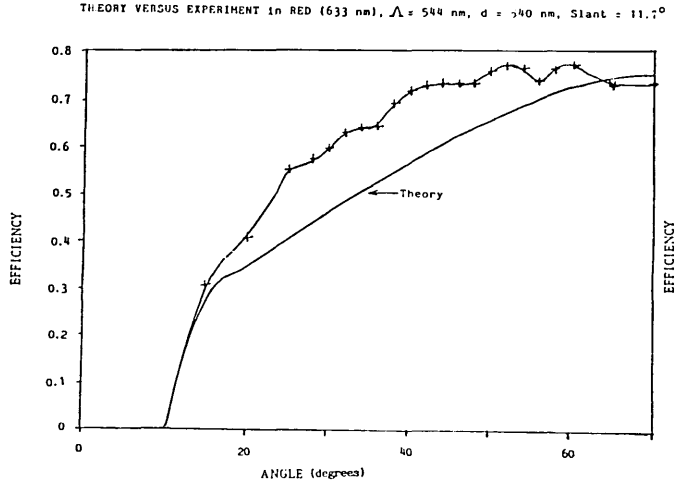

Fig 19 Grating 3 + = experimental (corrected) 1st order

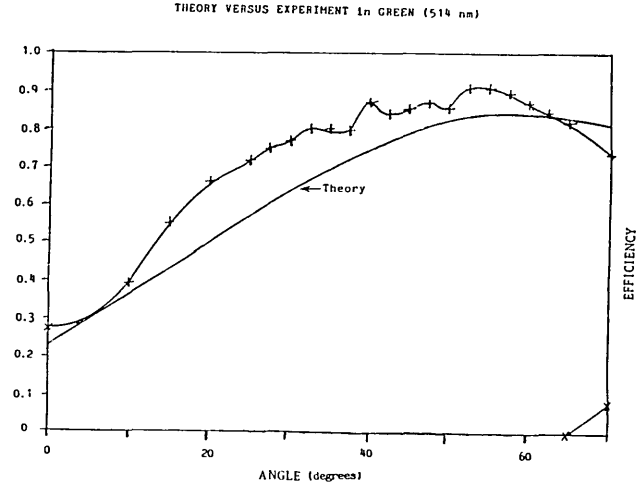

Fig. 20 Grating 3 + = experimental (corrected) 1st order, × = second order

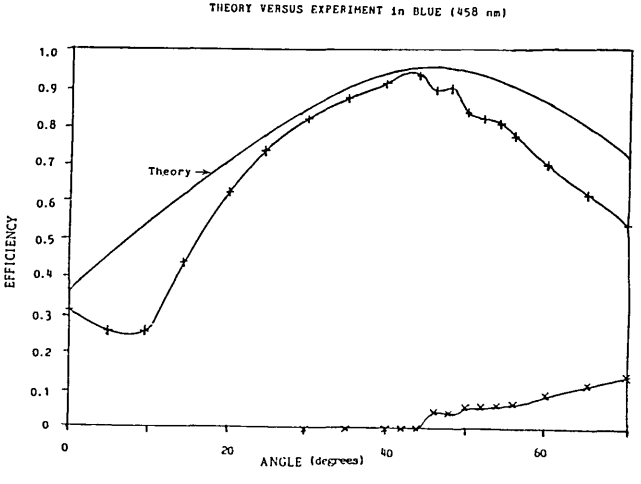

Fig. 21 Grating 3 + - experimental (corrected) 1st order, × - second order

the shorter wavelength in Fig. 5 the −1 order and +2 order have non-negligible intensity.

The data were compared with data generated by a computer program using Kogelnik's formulas for lossless dielectrics with arbitrary slant. The input parameters were measured quantities, namely, the grating spacing Λ and the depth d, defined as the top-to-bottom distance measured from the electron microscope photographs Figs. 1–3. The average refractive index of the grating was taken as 1.33, since the refractive index of the photoresist averages to 1.66 in the visible,[14] and for the modulation parameter n_1 was taken as 0.33, namely, half the difference between the refractive index difference between photoresist and air.

The results of these calculations are compared to the data corrected for reflection losses and absorption and shown for the three colors and three gratings in Figs. 7–9, 13–15, and 19–21.

VI. Discussion of Data Analysis

Looking at the nine comparison graphs, one notices a fair agreement between the experiments (somewhat corrected, mainly for reflection losses) and the theory, the latter with no adjusted parameter. The theory is certainly a useful guide in predicting grating behavior. However, the fit is clearly not perfect; in particular, deviations are important when a higher-order beam appears. Thus, for grating 1, the agreement becomes progressively worse for shorter wavelengths. This is not surprising since Kogelnik ignores higher-order beams in his volume hologram treatment, while for our gratings these do occur to some extent, particularly far from the Bragg condition and for short wavelengths. Grating 2 is shallower and has as a result observed and calculated efficiencies of ~50% instead of near 90% as for grating 1. Its efficiency increases with decreasing wavelength as expected since for the shorter wavelength the grating appears deeper than for the longer one. There is not much Bragg angle effect and also little of other-order beams so that the moderate efficiency is maintained over a large angular range, from 0 to 70° in Fig. 15. Grating 3, the deep slanted one, shows a very satisfying agreement between experiment and theory as is seen in Figs. 19–21.

The fit between experiment and theory is clearly far from perfect, but we feel that this relatively simple theory is quite useful as a guide in designing narrow spaced highly efficient, slanted relief gratings so that mainly one diffracted order occurs. Kogelnik's theory certainly fits much better than the thin phase grating theory, which fits none of the three gratings at all. The latter predicts that the efficiency for a sinusoidal grating cannot exceed the square of the maximum of the first-order Bessel function,[1] which is 33.9% for a sinusoidal or 40.4% for a square wave profile. All the gratings shown here are more or much more efficient than that. Consequently, although the gratings are in the intermediate region between thin and thick gratings,[7–9] they can be described reasonably well with the two-wave theory which is strictly applicable in the thick Bragg regime and they cannot be described at all with Bessel functions, used in the thin Raman-Nath regime.

Two parameters have often been used to define whether a grating is thin or thick; namely,

$$Q = \frac{2\pi\lambda d}{\bar{n}\Lambda^2 \cos\Theta},$$

and the modulation parameter,

$$\gamma = \frac{\pi n_1 d}{\lambda \cos\Theta},$$

where λ is the free space wavelength; d, the grating thickness; $\bar{n}$, the average refractive index; Λ, the grating spacing; Θ, the angle of the incident beam (inside the material) with the grating normal; and n_1, the amplitude of the refractive index modulation. The Electrical Engineering School at the Georgia Institute of Technology has developed criteria to determine whether one is in the thick or thin regime in a series of theoretical papers. Using the values for the parameters given in Sec. III, taking $\bar{n}$ as 1.33 and $\cos\Theta \sim 1$, one gets for the three gratings, taking as λ the value for the periodicity Λ,

$$Q_1 = 4.7, \gamma_1 = 1.0; \quad Q_2 = 3.2, \gamma_2 = 0.7; \quad Q_3 = 4.7, \gamma_3 = 1.0.$$

This places the gratings in the middle of the intermediate regime.[7] It is interesting and not surprising that the modulation parameter γ, which is given the symbol ν in Kogelnik's work, was found to give efficiencies near 90–95% when d/Λ is between 1.5 and 1.6 for the profiles obtained with the photoresist.[11] This agrees with Kogelnik's γ value of $\pi/2 = 1.57$ for 100% efficiency. Our graphs Figs. 9, 21, show that for gratings 1 and 3 the maximum efficiency is reached for violet light with $\gamma = 1.4$ and 1.2, respectively. At the same time, for the short violet wavelength other orders than only the first order are allowed, and, when they occur, they rob the first-order diffracted beam of its intensity and reduce the agreement between experiment and theory.

It appears that notwithstanding the considerable amount of useful work done to define the terms thin and thick gratings, there remains a certain amount of qualitative ambiguity in these expressions, not unlike in their ordinary life usage.

VII. Conclusions

Optical data of various photoresist relief type diffraction gratings are presented. Even though the parameters of these gratings place them within what is usually referred to as the intermediate region, between thin and thick gratings, we have shown that Kogelnik's coupled-wave theory, strictly applicable to thick volume gratings, serves as a useful guide to predict and thus control the optical properties of these types of grating.

A practical use of these gratings is the high diffraction efficiency they show over a wide range of incidence angles and wavelengths, thus combining the best of the two regimes, thick and thin, between which they fall.

The authors want to thank William Ziemer for his expert help in making the electron microscope photographs and performing some of the measurements, and the Department of Energy, through the Advanced Environmental Research Group, for their support of this work.

References

1. R. J. Collier, C. B. Burckhardt, and L. H. Lin, *Optical Holography* (Academic Press, New York, 1971), pp. 261 and 268.

2. R. A. Bartolini, "Characteristics of Relief Phase Holograms Recorded in Photoresists," Appl. Opt. **13,** 129–139 (1974).
3. H. Kogelnik, "Coupled Wave Theory for Thick Hologram Gratings," Bell Syst. Tech. J. **48,** 2909–2947 (1969).
4. C. J. Kramer, "Hologon Laser Scanners for Nonimpact Printing," Proc. Soc. Photo-Opt. Instrum. Eng. **390,** 165–170 (1982).
5. R. C. Enger and S. K. Case, "High Frequency Holographic Transmission Gratings in Photoresist," J. Opt. Soc. Am. **73,** 1113–1118 (1983).
6. M. G. Moharam, T. K. Gaylord, G. T. Sincerbox, H. Werlich, and B. Yung, "Diffraction Characteristics of Photoresist Surface-Relief Gratings," Appl. Opt. **23,** 3214–3220 (1984).
7. R. Magnusson and T. K. Gaylord, "Diffraction Regimes of Transmission Gratings," J. Opt. Soc. Am. **68,** 809–814 (1978).
8. M. G. Moharam, T. K. Gaylord, and R. Magnusson, "Criteria for Bragg Regime Diffraction by Phase Gratings," Opt. Commun. **32,** 14–18 (1980); "Criteria for Raman-Nath Regime Diffraction by Phase Gratings," Opt. Commun. **32,** 19–23 (1980).
9. T. K. Gaylord and M. G. Moharam, "Thin and Thick Gratings: Terminology Clarification," Appl. Opt. **20,** 3271–3273 (1981).
10. R. Magnusson and T. K. Gaylord, "Analysis of Multiwave Diffraction of Thick Gratings," J. Opt. Soc. Am. **67,** 1165–1170 (1977).
11. M. G. Moharam and T. K. Gaylord, "Diffraction Analysis of Dielectric Surface-Relief Gratings," J. Opt. Soc. Am. **72,** 1385–1392 (1982).
12. M. G. Moharam and T. K. Gaylord, "Three-Dimensional Vector Coupled-Wave Analysis of Planar-Grating Diffraction," J. Opt. Soc. Am. **73,** 1105–1112 (1983).
13. L. Solymar and D. J. Cooke, *Volume Holography and Volume Gratings* (Academic Press, London, 1981).
14. H. J. Gerritsen, "Dispersion Effects in Relief Holograms Immersed in Near Index Matched Liquids or Christiansen Revisited," Appl. Opt. **25,** 2382–2385 (1986).